INFECTION AND IMMUNITY, Mar. 2005, p. 1811–1819 Vol. 73, No. 3
0019-9567/05/$08.00+0 doi:10.1128/IAI.73.3.1811–1819.2005

Biofilm Formation, *icaADBC* Transcription, and Polysaccharide Intercellular Adhesin Synthesis by Staphylococci in a Device-Related Infection Model

Ursula Fluckiger,[1] Martina Ulrich,[2] Andrea Steinhuber,[1] Gerd Döring,[2] Dietrich Mack,[3]† Regine Landmann,[1] Christiane Goerke,[2] and Christiane Wolz[2]*

Division of Infectious Diseases and Department of Research, University Hospital, Basel, Switzerland,[1] and Institute of Medical Microbiology and Hygiene, University of Tübingen, Tübingen,[2] and Institut für Infektionsmedizin, Universitätsklinikum, Hamburg-Eppendorf,[3] Germany

Received 20 April 2004/Returned for modification 13 July 2004/Accepted 4 November 2004

Biofilm formation of *Staphylococcus epidermidis* and *S. aureus* is mediated by the polysaccharide intercellular adhesin (PIA) encoded by the *ica* operon. We used a device-related animal model to investigate biofilm formation, PIA expression (immunofluorescence), and *ica* transcription (quantitative transcript analysis) throughout the course of infection by using two prototypic *S. aureus* strains and one *S. epidermidis* strain as well as corresponding *ica* mutants. During infection, the *ica* mutants were growth attenuated when inoculated in competition with the corresponding wild-type strains but not when grown singly. A typical biofilm was observed at the late course of infection. Only in *S. aureus* RN6390, not in *S. aureus* Newman, were PIA and *ica*-specific transcripts detectable after anaerobic growth in vitro. However, both *S. aureus* strains were PIA positive in vivo by day 8 of infection. *ica* transcription preceded PIA expression and biofilm formation in vivo. In *S. epidermidis*, both PIA and *ica* expression levels were elevated compared to those in the *S. aureus* strains in vitro as well as in vivo and were detectable throughout the course of infection. In conclusion, in *S. aureus*, PIA expression is dependent on the genetic background of the strain as well as on strong inducing conditions, such as those dominating in vivo. In *S. epidermidis*, PIA expression is elevated and less vulnerable to environmental conditions.

The success of the increasing number of artificial-joint replacements and other implanted devices is hampered by device-related infections. Prosthetic-device infections are enormously costly for the community and disabling for the individual patient. Infections can occur during the surgical procedure or hematogenously, even years after the implantation. The staphylococci *Staphylococcus epidermidis* and *S. aureus* account for more than half of prosthetic-device-associated infections (51, 58). *S. aureus* adheres primarily to the device via cell wall-attached adhesins that recognize host proteins coating biomaterial surfaces soon after implantation (15). In contrast, adhesins of *S. epidermidis* are less well characterized, but initial adherence is probably multifactorial, involving, among other factors, the autolysins AtlE, Embp, and Fbe (26, 34). After initial adherence, biofilm formation occurs by bacterial accumulation mediated by extracellular polysaccharides.

Biofilm formation was first characterized in *S. epidermidis* on a molecular level. Biofilm development requires the polysaccharide intercellular adhesin (PIA), which is synthesized by enzymes encoded by the *ica* operon (27, 35–37). *S. epidermidis* forms biofilm on nearly all kinds of medical devices and implants (reviewed in reference 25). Furthermore, the relevance of PIA production in the pathogenesis of *S. epidermidis* in human infections is emphasized by several studies showing that infecting strains are significantly more *ica* positive than colonizing strains (3, 4, 9, 18, 19, 42, 57). In addition, the role of PIA as an important virulence factor for *S. epidermidis* was demonstrated in two different animal models (48–50).

Recently, it was found that the *ica* locus is conserved between *S. epidermidis* and *S. aureus* (7, 41). Interestingly, in contrast to *S. epidermidis*, PIA production and biofilm formation in vitro is less pronounced in most *S. aureus* strains and often observed only under stringent in vitro conditions, such as low oxygen (8). Analysis of clinical *S. aureus* isolates from prosthetic-joint infections, bacteremia, or catheter-related infections showed the presence of the *ica* locus in most isolates but a lack of PIA production in a varying percentages of these strains in vitro (1, 7, 8, 16, 30, 40, 44, 47). The circumstances leading to the formation of biofilm in *S. aureus* infections are not clearly understood and are difficult to derive from in vitro results. However, antibodies against PIA proved to be protective in mice, emphasizing a role of PIA for virulence also in *S. aureus* (41).

We aimed to analyze PIA expression from *S. aureus* and *S. epidermidis* during the course of infection by using a device-related animal model. Growth and adherence of the *ica*-deficient mutants from both species did not differ from that in the

* Corresponding author. Mailing address: Institut für Medizinische Mikrobiologie und Hygiene, Wilhemstr. 31, 72074 Tübingen, Germany. Phone: 49 7071 2980187. Fax: 49 7071 293011. E-mail: Christiane.Wolz@uni-tuebingen.de.

† Present address: Medical Microbiology and Infectious Diseases, The Clinical School, University of Wales Swansea, Swansea, United Kingdom.

isogenic parental strains when the animals were grown in separate cages. However, in competition infection, the wild-type strains hindered the mutant strains from growing up to the same density. *S. epidermidis* was already PIA positive at the onset of infection. *S. aureus* strain RN6390 as well as the in vitro biofilm-negative strain Newman became PIA positive only in the later stages of infection.

MATERIALS AND METHODS

Bacterial strains and growth conditions. The following strains were used for analysis: *S. epidermidis* strain 1457 and its isogenic *ica* mutant (36), *S. aureus* strain Newman (13) and *S. aureus* strain RN6390 (45) and their corresponding isogenic *ica*-deficient derivatives CW25 (Newman Δ*ica*::*tet*) and CW26 (RN6390 Δ*ica*::*tet*), and the *agr* mutant strains RN6911 (RN6390 Δ*agr*::*tet*) (45) and ALC355 (Newman Δ*agr*::*tet*) (55). For in vivo experiments, staphylococci were grown overnight in Casamino Acids–yeast extract–β-glycerophosphate–glucose medium (CYPG) (43) with aeration, washed three times in sterile NaCl (0.9%), and diluted to the desired inoculum size of approximately 5×10^5 CFU/ml. For in vitro analysis, bacteria from an overnight culture were diluted to an initial optical density at 600 nm (OD_{600}) of 0.05 and grown with shaking at 37°C to the mid-exponential phase (OD_{600} = 0.8 at time 1), to the post-exponential phase (OD_{600} = 8 at time 3), or for 24 h to the stationary phase. For analysis of PIA expression by immunofluorescence, bacteria were grown anaerobically on chamber slides in tryptic soy broth containing 1% glucose for up to 48 h (8). Biofilm formation in vitro was assessed in a microtiter plate assay as described previously (5).

Construction of *ica* mutant strains. A Φ11 lysate of the *ica* deletion mutant ATCC 35556 Δ*ica*::*tet* (7) was used to transduce strain Newman and strain RN6390. Tetracycline-resistant transductants were selected, and the *ica* gene replacement was verified by PCR. Oligonucleotides were chosen to allow amplification of the following fragments in the transductants and the original *ica* deletion mutants corresponding to the *tet* insertion site within the *ica* operon: CTTCGATGTCGAAAATAAACTC based on *ica* and GCTTCTGGAATGAG TTTGCT based on *tet*. Southern hybridization was performed on SmaI-digested chromosomal DNA after pulsed-field gel electrophoresis using *ica*-specific probes.

Animal model of device-related infection. The well-established guinea pig and mouse models of implant infection were used (31, 32, 59). Four perforated Teflon tubes filled with eight pieces of plastic catheter were inserted in the flanks of the animals. Two weeks after implantation, approximately 2×10^5 to 3×10^5 CFU of the test strain was inoculated into the tissue cages.

Before inoculation, the interstitial fluid, which had accumulated in the tissue cages, was checked for sterility. Animals infected with *S. epidermidis* were sacrificed 2, 4, 6, 8, 12, or 16 days after bacterial challenge. Those animals infected with *S. aureus* were sacrificed at days 2, 4, 6, and 8 only because increasing inflammation and abscess formation around the tissue cages limited the duration of the experiment. Every second day after bacterial challenge, 1 aliquot of aspirated exudate was taken and immediately stored in liquid nitrogen for subsequent RNA preparation. A second aliquot was used for quantitative bacteriology. The tissue cages were removed from sacrificed animals, and three pieces of catheter were used to count the adherent bacteria (see following paragraph). Two pieces were fixed with 2.5% glutaraldehyde for microscopy. Each strain was tested in at least three independent animal experiments performed on different days.

For competition experiments, wild-type and *ica* mutant strains were inoculated into implanted tissue cages in mice at a ratio of 1:1 or 1:100. The coinfection was maintained for 8 days with CFU determinations of the exudates at days 2 and 8, as described above.

Bacterial quantification in vitro and in vivo. Serial dilutions of broth culture and of aspirated exudates from the infected-animal cages were plated onto blood agar plates (tryptic soy agar containing 5% sheep blood). For CFU determinations of the competition experiments, serial dilutions of bacteria were plated in parallel on tryptic soy agar with or without the appropriate selective antibiotic, erythromycin (10 μg/ml) for *S. epidermidis* and tetracycline (3 μg/ml) for *S. aureus*, to determine the ratio of mutant (Erm^r to Tet^r, respectively) to wild-type (Erm^s to Tet^s, respectively) bacteria. In addition, we subcultivated 100 randomized colonies of each exudate sample from nonselective plates on erythromycin and tetracycline plates, respectively, to verify the ratios of wild-type to *ica* mutant CFU in the mixed infections. The number of bacteria adhering to the plastic catheters was determined as described previously (54). Briefly, for each time point, three pieces of catheter were washed twice with saline and each catheter was placed in a tube with 1 ml of 0.9% NaCl containing EDTA (0.15%) and Triton X-100 (0.1%). The tubes were vigorously vortexed three times for 15 s. The tubes were then placed in an ultrasonic bath and sonicated for 3 min at 120 W. After an additional mixing step, 100 μl of the liquid was diluted for quantitative bacterial culture on blood agar plates. Stability of the mutant strains was confirmed by subculturing of the strains on plates containing tetracycline (3 μg/ml) or erythromycin (10 μg/ml).

PIA detection by indirect immunofluorescence in vivo and in vitro. PIA production in vivo was determined in exudates which were mixed with the same volume of 8% paraformaldehyde immediately after aspiration, diluted 1:10 with phosphate-buffered saline (PBS) for *S. aureus*, concentrated 10 times for *S. epidermidis*, and spotted on poly-L-lysine-coated slides. PIA production in vitro was determined in planktonic bacteria and in bacteria forming a biofilm on poly-L-lysine coated chamber slides after anaerobic growth for 48 h. For PIA-specific immunofluorescence, the bacteria were fixed with 4% formaldehyde for 10 min at room temperature. The slides were washed three times with PBS-Tween and incubated with human serum (1:10 in PBS) for 30 min to prevent unspecific binding of immunoglobulin G by cell wall-associated protein A. The slides were incubated with a PIA-specific polyclonal antiserum from rabbit (1:100 in PBS-Tween) for 1 h, followed by incubation of Cy3-conjugated anti-rabbit $F(ab)_2$ fragment (1:100 in PBS-Tween; Dianova) for 1 h. Bacteria were also stained with 4′,6′-diamidino-2-phenylindole (DAPI; 2 μg/ml) for 5 min, washed three times with water, and air dried. The slides were then mounted with fluorescent mounting medium (Dako), and positively stained bacteria were detected using fluorescence microscopy. Experiments were repeated three times at different time intervals.

Scanning electron microscopy (SEM). Pieces of catheter material were fixed with 2.5% glutaraldehyde, dried, and sputtered with gold to analyze adherence and biofilm formation by electron microscopy.

RNA isolation. For RNA isolation from culture, bacteria were grown in CYPG to the desired growth phase. A pellet of approximately 5×10^9 bacteria was then resuspended in 1 ml of Trizol reagent (Gibco BRL, Life Technologies), and the mixture was disrupted with 0.5 ml of zirconia-silica beads in a high-speed homogenizer (Savant Instrument, Farmingdale, N.Y.). Total RNA was isolated as directed in the instructions provided by the manufacturer of Trizol. For RNA preparation from exudates, the frozen samples were thawed rapidly and 200-μl aliquots were used. RNA was isolated and purified as described previously (24). Contaminating DNA was degraded by digesting RNA samples with DNase as described previously (23).

Quantification of specific transcripts with LightCycler RT-PCR. Specific RNA standards for the quantification of *gyr* and *ica* were engineered as described elsewhere (22). LightCycler reverse transcription (RT)-PCR was carried out using the LightCycler RNA amplification kit for hybridization probes (Roche Biochemicals, Basel, Switzerland). Master mixes were prepared following the manufacturer's instructions by using the oligonucleotides specific for *gyr* and *ica* (Table 1). After RT for 20 min at 50°C, the following temperature profile was utilized for amplification: denaturation for 1 cycle at 95°C for 30 s and for 45 cycles at 95°C for 1 s (temperature transition of 20°C/s), at 55 to 50°C (step size of 1°C, step delay of 1 cycle) for 15 s (temperature transition 20°C/s), and at 72°C for 15 s (temperature transition of 2°C/s) and fluorescence acquisition at 55 to 50°C in single mode. Melting curve analysis was performed at 45 to 90°C (temperature transition of 0.2°C/s) with stepwise fluorescence acquisition. Sequence-specific standard curves were generated using 10-fold serial dilutions (10^4 to 10^8 copies/μl) of the specific RNA standards. The number of copies of each sample transcript was then determined with the aid of the LightCycler software. The specificity of the PCR was verified by size determination of the amplicons by agarose gel electrophoresis.

Statistics. The results are expressed as mean values ± standard deviations. Statistical analysis was performed by Student's two-tailed test. A P value of <0.05 was considered significant.

RESULTS

Biofilm formation in the animal model. *S. aureus* strains RN6390 and Newman were inoculated after sterile implantation of the tissue cages containing pieces of catheters. To evaluate biofilm formation on the catheter pieces in vivo, the tissue cages were explanted 8 days after inoculation. Pieces of catheters were washed with sterile saline and prepared for SEM analysis (Fig. 1). SEM showed bacterial

TABLE 1. Oligonucleotide primers and LightCycler hybridization probes

Target gene	GenBank accession no.	Primer	Sequence[a]
S. aureus icaA	AF086783	*icaU*	TGGCTGTATTAAGCGAAGTC
		icaL	TTCCAAAGACCTCCCAATGT
		icaFL	TGTCGACGTTGGCTACTGGGAT-FL
		icaLC	Red640-CTGATATGATTACCGAAGATATTGCAGT-ph
S. aureus gyr	D10489	*gyrU*	TTATGGTGCTGGGCAAATACA
		gyrL	CACCATGTAAACCACCAGATA
		gyrFL1	ATTTTAACTGTTTTACATGCTGGTGGTAA-FL
		gyrLC1	Red640-TTTGGCGGTGGCGGATACA-ph
S. epidermidis icaA	U43366	*Epi-icaU*	CAATCTCTTGCAGGAGC
		Epi-icaL	CTTGAGCCCATCGAACC
		Epi-icaFL1	CAAAGATGTAGGTTATTGGGATACTGACA-FL
		Epi-icaLC1	Red640-ATTACTGAGGATATTGCTGTTTCATGGA-ph
S. epidermidis gyr	AF314404	*Epi-gyrU*	GGTATGTATATTGGTTCAACTTCAG
		Epi-gyrL	GTGAAGACCGCCAGAT
		Epi-gyrFL2	GGGTTGCACCATTTAGTATGGGAAA-FL
		Epi-gyrLC2	Red640-TGTTGATAATAGTATTGACGAGGCATTAGC-ph

[a] FL, fluorescein; Red640, LightCycler Red640-*N*-succinimide ester; ph, 3′-phosphate.

clusters attached to the catheter in close contact to host cells and cellular debris. Additionally, uptake of bacteria by surface-attached phagocytes could be observed (Fig. 1B). These images demonstrate *S. aureus* biofilm formation in the animal model of device-related infections. There were no obvious differences between cages infected with either strain Newman or strain RN6390. Due to the lower bacterial number of *S. epidermidis* cells in vivo, biofilm could not be visualized using SEM.

Biofilm formation and PIA expression in vitro. Prototypic *S. epidermidis* as well as *S. aureus* strains were grown anaerobically on chamber slides for 48 h in tryptic soy broth with 1% glucose to get maximum PIA expression (8), reflecting the in vivo situation where low oxygen might be present in a late stage of localized infection. Accordingly, *S. epidermidis* and *S. aureus* strain RN6390 were clearly PIA positive by immunofluorescence using PIA-specific antiserum (Fig. 2C and E). In contrast, in *S. aureus* strain Newman, no PIA production could be detected. Additionally, in a microtiter plate assay, no biofilm formation could be observed in strain Newman. To analyze whether this was due to the proposed inhibitory action of the *agr* operon (53), isogenic *agr*-deficient mutants were also analyzed. As expected, biofilm formation was increased in the *agr*-deficient derivative of strain RN6390 (RN6911). However, deletion of *agr* in strain Newman did not enhance biofilm formation or PIA expression (data not shown). These results indicate that, in strain Newman, PIA expression is severely down-regulated in vitro. Since both *S. aureus* strains tested (RN6390 and Newman) were able to form biofilms in the tissue cage model (Fig. 1), we aimed to analyze the PIA expression of these two strains in vivo in more detail.

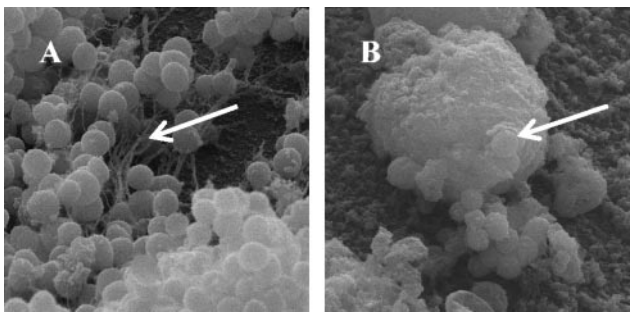

FIG. 1. SEM micrographs of *S. aureus* RN6390 (A) and *S. aureus* Newman (B) adhering to catheter pieces explanted into tissue cages. Microcolonies (arrows) of staphylococci were found attached to the catheters. Engulfment of staphylococci by a phagocytic cell was observed (panel B, arrow). Original magnification, ×10,560.

Construction of *ica* mutants of strain RN6390 and Newman. In order to obtain PIA-negative control strains, we first constructed *ica* mutants of the two *S. aureus* strains RN6390 and Newman. The replacement of the *ica* operon by *tet* in the transductants was confirmed by PCR. From the *ica* mutants, a PCR amplicon corresponding to the *tet* insertion site within *ica* could be amplified. The restriction fragment patterns obtained by pulsed-field gel electrophoresis differed between the mutants and the corresponding parental strains only in one fragment, which could be shown to encompass the *ica* locus. By Southern blotting, the fragments in the mutant strains did not react with a DNA probe specific for *icaA*. Additionally, both mutants were shown to be PIA negative in vitro as well as in vivo using PIA-specific antibodies (Fig. 2 and 4).

Bacterial growth curves and adherence in vivo. First, the growth and adherence capabilities of *S. aureus* and *S. epidermidis* strains and their *ica* mutants in the animal model were assessed. Implanted tissue cages containing catheters were inoculated with approximately 5×10^5 CFU/cage (Fig. 3A). *S. aureus* strains RN6390 and Newman and their *ica* mutants grew up to 1.4×10^8 to 4.5×10^8 CFU/ml in tissue cages 8 days after infection. At 2, 6, and 8 days after inoculation, wild-type strains and their *ica*-deficient mutants reached similar CFU counts. At day 6, the numbers of both *S. aureus* wild-type and *ica* mutant strains reached a maximum of about 10^8 CFU/ml

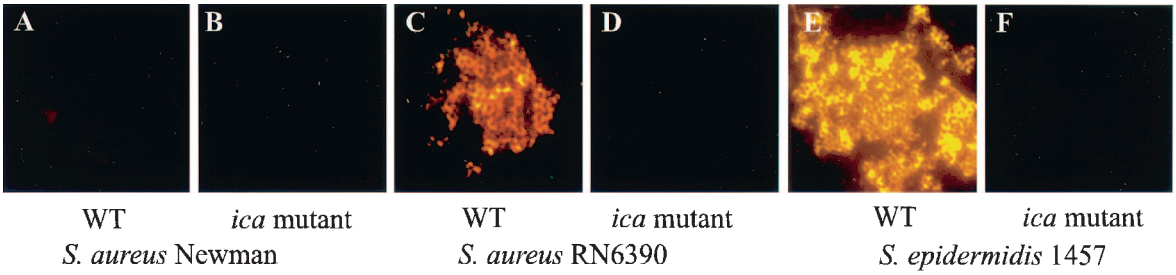

FIG. 2. *S. aureus* Newman, *S. aureus* RN6390, *S. epidermidis* 1457, and their *ica* mutants were grown anaerobically in chamber slides for 48 h. In panels A through F, culture broth was stained by indirect immunofluorescence to detect PIA. PIA was not detected in *S. aureus* strain Newman (panel A). In contrast, PIA was strongly marked by immunofluorescence in strain *S. aureus* RN6390 (panel C) and *S. epidermidis* 1457 (panel E) under anaerobic in vitro growth. All three *ica* mutants (panels B, D, and F) were PIA negative. WT, wild type. Original magnification, ×1,000.

(range, 8×10^7 to 2×10^8 CFU/ml) and remained stable up to day 8. No significant differences in growth for wild-type strains and their *ica* mutants was observed at day 8 ($P = 0.92$ for *S. aureus* RN6390, $P = 0.73$ for *S. aureus* Newman; Student's *t* test).

CFU counts of *S. epidermidis* strains were maintained at about 5×10^5 CFU/ml throughout the course of infection up to 12 days. Thereafter, wild-type *S. epidermidis* and the *ica* mutant decreased 1 log to 2×10^4 to 4×10^4 CFU/ml.

Figure 3B shows the bacterial counts on the catheters within the tissue cages. As for the exudates, the bacterial counts of *S. epidermidis* were lower than those of *S. aureus*. The 2-day CFU counts of the adherent bacteria differed between the wild-type strains and the corresponding *ica* mutants. However, at 8 days, there was no significant difference between the wild-type strains and their *ica* mutants. The average CFU counts were between 2×10^4 and 3×10^5/piece of catheter for adhering *S. aureus* Newman and 4×10^4 to 5×10^4/piece of catheter for *S. aureus* RN6390; for *S. epidermidis* 1457, the count varied between 3×10^4 and 6×10^4 CFU/piece of catheter. According to the decreasing CFU in exudate, the adhering bacteria of *S. epidermidis* and its *ica* mutant decreased to very low numbers of 100 to 500 CFU/piece of catheter at 16 days.

To determine whether *ica*-positive and *ica*-deficient strains inoculated together in the same cage exhibit the same growth capabilities, we performed competition experiments (Fig. 4). The ratios of wild type to mutant were 1:1 (Fig. 4A and C) and 1:100 (Fig. 4B and D), respectively. As observed in growth curves for single-strain infections, the CFU of mixed *S. epidermidis* infections declined during the first 2 days independent of the inoculum ratio. Thereafter, the *S. epidermidis* strain lacking the *ica* locus grew slower than the wild type; however, the mutant was not completely cleared. In cages infected with *S. aureus* wild type and *ica* mutants at a ratio of 1:1, the mutant strain grew slower than the wild type at 2 and 8 days (Fig. 4C). However, an inoculum of the *ica* mutant which was 100 times higher than that of the wild-type *S. aureus* resulted in a similar CFU count after 8 days (Fig. 4D).

PIA expression in vivo determined using immunofluorescence microscopy. Next, we examined aspirated exudates from tissue cages by indirect immunofluorescence in order to investigate the production of PIA during the course of infection. There was a marked difference of PIA production between *S. aureus* and *S. epidermidis*. Figure 5 illustrates the three tested parental strains and their respective *ica* mutants. For each time point, two pictures are shown. In the upper panels, the exudates are stained by immunofluorescence to detect PIA,

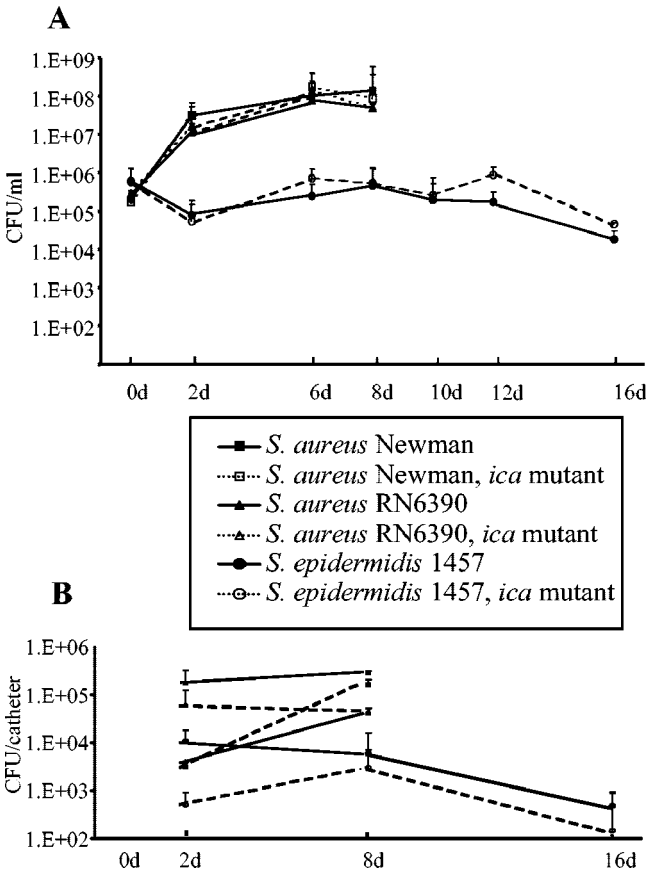

FIG. 3. In vivo growth curves of *S. aureus* RN6390, *S. aureus* Newman, *S. epidermidis* 1457, and their isogenic *ica* mutants in the guinea pig model. (A) Number of viable counts (CFU/ml) in exudates of tissue cages at the time of bacterial challenge at 0 days (0d), 2d, 6d, and 8d after *S. aureus* inoculation and 2d, 6d, 8d, 10d, 12d, and 16d after *S. epidermidis* inoculation. Each value is the mean ± standard deviation for six to eight cages from three or four independent experiments. (B) Number of bacteria attached to the catheters in the tissue cages at 2d and 8d after inoculation with *S. aureus* RN6390 or *S. aureus* Newman and additionally at 16d after *S. epidermidis* 1457 inoculation. Each value is the mean ± standard deviation for six to eight cages from three independent experiments.

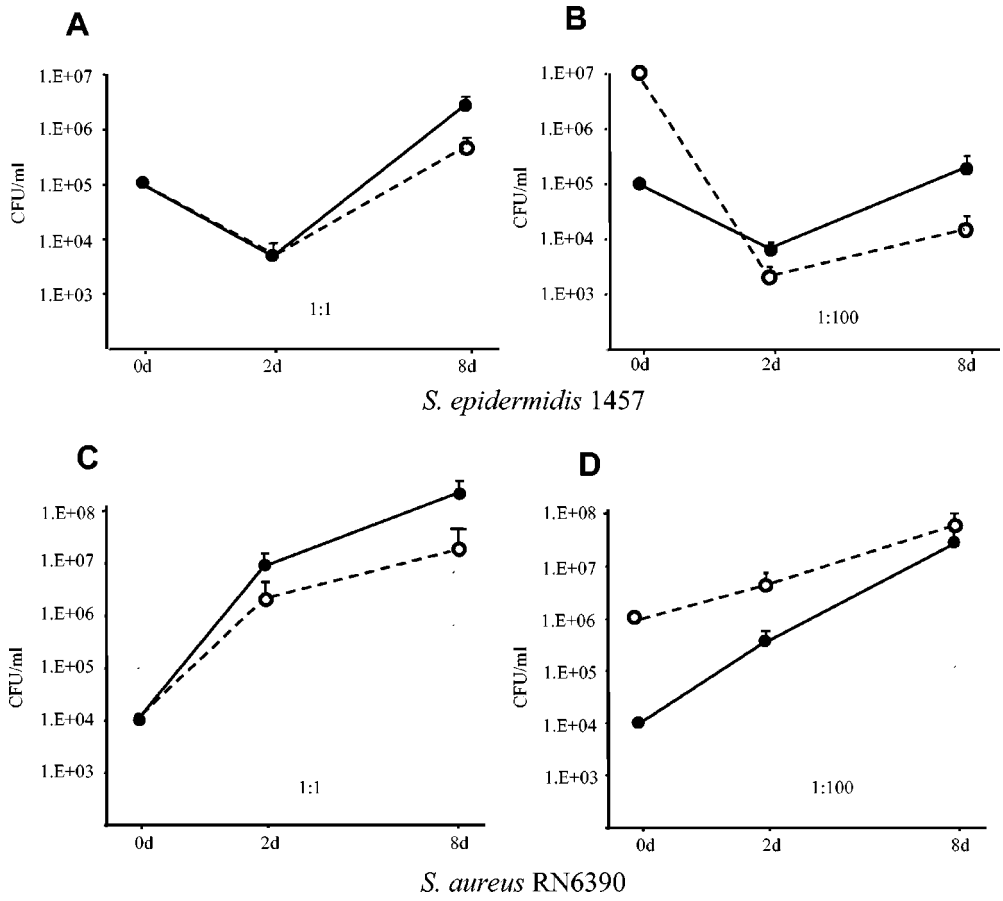

FIG. 4. In vivo growth curves of *S. epidermidis* 1457 (A and B) and *S. aureus* RN 6390 (C and D) and their respective *ica* mutants injected together into the tissue cages of mice at ratios of 1:1 (left panels) and 1:100 (right panels). Numbers of viable counts (CFU/ml) at the time point of infection, at day 2 (2d), and at 8d postinfection are shown. Solid lines represent the wild-type strains, and dotted lines represent the *ica* mutants. Data from three to eight mice from two experiments were pooled. At 2d, CFU counts of the *ica*-deficient *S. aureus* strains were lower than those of the wild-type strains, but this was not the case for *S. epidermidis*. At 8d, the *ica* mutants of both *S. epidermidis* and *S. aureus* reached significantly lower CFU counts than the corresponding wild-type strains ($P < 0.05$).

whereas the lower panels show pictures of the corresponding exudates stained with DAPI to identify the bacteria. In both *S. aureus* strains, PIA was negative in aspirated exudates 2 days after inoculation but clearly positive at day 8 (Fig. 5A through C and E through G). Exudates of the *ica* mutants of both *S. aureus* strains and *S. epidermidis* were PIA negative at each of the tested time points (shown only at day 8 [Fig. 5D, H, and M]). In contrast, in *S. epidermidis* 1457, PIA was detected by immunofluorescence already at the second day after bacterial inoculation (Fig. 5I). Bacteria were detected as pairs in the early course of infection and as large cell clusters at day 16 (Fig. 5I and L, respectively).

Transcription of *ica* in vitro and in vivo. In order to investigate whether PIA expression correlates with transcription of the *ica* operon, quantitative RT-PCR was performed using bacteria from in vitro cultures and directly from the exudates without subculturing (Fig. 6). In vitro *S. aureus* RN6390 and *S. aureus* Newman showed similar patterns, with increasing transcription levels at time 3 (late-exponential-growth phase) compared to those at time 1 (mid-exponential-growth phase) and decreasing levels at 24 h. At all three time points, the ratio of copy numbers of *ica* relative to those of the reference transcript *gyr* (*y* axis; copies of *ica* per copy of *gyr*) was lower in strain Newman than in strain RN6390. This finding is in close agreement with the immunofluorescence data, where PIA was detectable in vitro only in strain RN6390, not in strain Newman.

In contrast to the in vitro situation, the *ica* transcript levels of *S. aureus* RN6390 and *S. aureus* Newman were similar in vivo at days 2 and 8, with 0.012 and 0.015 copy per copy of *gyr* at 2 days and 0.007 and 0.009 copy per copy of *gyr* at 8 days, respectively. In strain Newman, the *ica*/*gyr* mRNA ratios were higher in vivo than in vitro.

S. epidermidis showed a remarkable expression of *ica* transcripts in vitro, which were 3 logs above those found in the *S. aureus* strains grown under the same conditions. In vivo, we could detect *ica*-specific transcripts in the exudates of *S. epidermidis*-infected animals at copy numbers 2 logs higher than those of *S. aureus* after 2 days of infection, indicating a particularly high expression of *ica* already early in the infection course. The copy numbers remained 2 logs higher than those of *S. aureus* throughout the infection course.

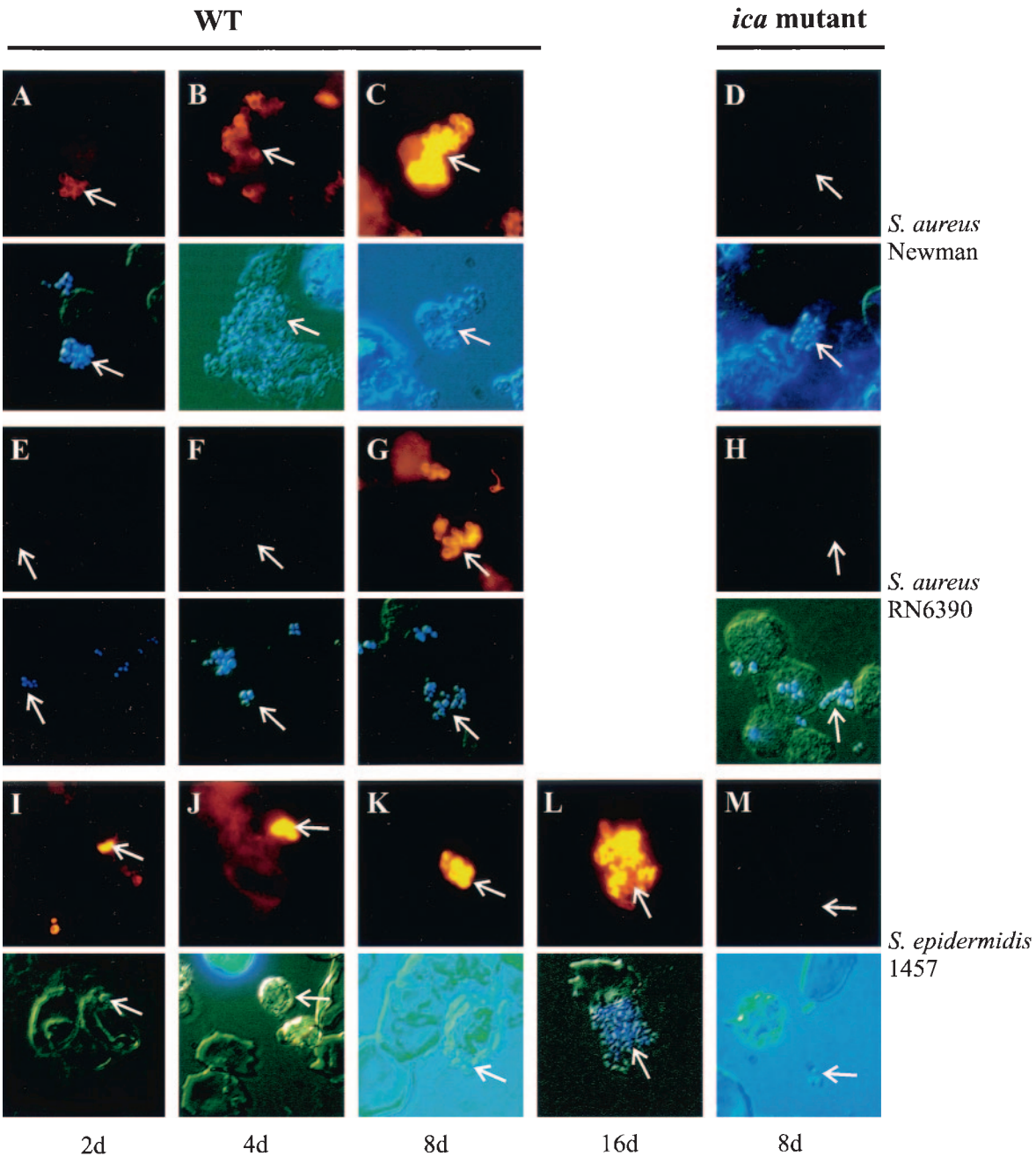

FIG. 5. Micrographs of *S. aureus* strains RN6390 (A through C) and Newman (E through G) in exudates aspirated at day 2 (2d), 4d, and 8d; *S. epidermidis* 1457 (I through L) aspirated at 2d, 4d, 8d, and 16d; and their respective *ica* mutants (D, H, and M) aspirated at 8d from in vivo tissue cages. Bacteria were stained by indirect immunofluorescence for the detection of PIA (upper panels for each locant, arrows) and with DAPI to show the presence of all bacteria (lower panels for each locant). Immunofluorescence micrographs of exudates for the detection of PIA were negative at 2d and 4d after inoculation. However, both *S. aureus* strains were clearly positive at 8d (panels C, G, and K). Aspirated exudates from infected tissue cages with *S. epidermidis* were PIA positive already 2d after infection (panel I). Both species appeared in clusters at 8d (panels C, G, and L). The *ica* mutants of all three tested strains remained PIA negative (panels D, H, and M). WT, wild type. Original magnification, ×1,000.

DISCUSSION

We could show that the device-related infection model is well suited to study biofilm formation during infection. Bacterial biofilms of *S. aureus* on pieces of catheter could be confirmed by SEM. These electron micrographs closely resemble those presented for biofilm-coated devices explanted from humans infected with staphylococci (11, 12). Additionally, PIA expression of *S. aureus* and *S. epidermidis* and formation of bacterial clusters probably reflecting biofilm formation could be demonstrated in the later course of infection by immunofluorescence.

Comparison of the *ica* transcription and PIA synthesis levels

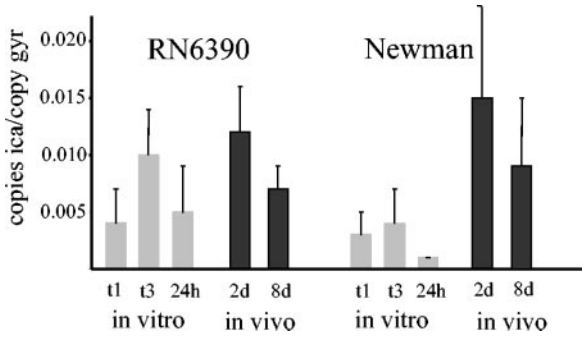

FIG. 6. Quantitative transcript analysis of *S. aureus* RN6390 and *S. aureus* Newman by LightCycler RT-PCR in vitro and in vivo. *ica* transcripts were quantified in relation to the number of *gyr* transcripts in each sample. Transcription of *ica* was determined in the mid-exponential phase (time 1 [t1]) and in the late-exponential phase (t3), as well as after 24 h of growth in CYPG (gray columns) and in exudates from infected devices in guinea pigs 2 days (2d) and 8d after bacterial inoculation (black columns). Values from three separate RNA preparations were used to calculate the mean values ± standard deviations.

of *S. aureus* strains revealed marked strain-dependent differences under in vitro but not in vivo conditions. In the in vitro experiments, *S. aureus* strain RN6390 produced PIA under an anaerobic condition after 48 h of inoculation whereas in *S. aureus* Newman, no PIA production was detectable. In contrast, under the in vivo condition, both *S. aureus* strains produced PIA late in the infection course, suggesting that PIA production is strongly induced in vivo. This confirms previous data showing that *S. aureus* bacteria are PIA positive during lung infection in patients suffering from cystic fibrosis (41). The signals resulting in PIA expression in *S. aureus* during the course of infection remain unknown. Numerous recent publications report on factors influencing PIA or biofilm production, such as glucose and other sugars, high osmolarity, and anaerobiosis (8, 21, 29, 30, 39, 46). It is conceivable that oxygen tension decreases in abscesses, as observed in *S. aureus*-infected cages, and this may trigger PIA formation in *S. aureus*. However, additional signals are obviously required, since we were unable to induce PIA formation in strain Newman under anaerobic conditions in vitro.

The regulatory circuits resulting in PIA expression are obviously different between the two species. The overall amount of PIA as well as of the *ica*-specific transcripts in *S. epidermidis* is elevated compared to that in the *S. aureus* strains. *S. epidermidis* was PIA positive under all conditions examined, whereas in *S. aureus*, PIA expression was dependent on the genetic background as well as on growth conditions. Regulatory loci which are known to be involved in PIA synthesis, such as *sarA*, *sigB*, and *icaR*, are conserved between *S. aureus* and *S. epidermidis* (2, 6, 14, 28, 38, 46, 52). However, one may assume that there are species-specific differences in their activity and function leading to the differences in the observed PIA expression.

We aimed to correlate the *ica* transcript levels detected by quantitative RT-PCR with PIA expression analyzed by immunofluorescence in vitro and in vivo. The *ica* transcription as well as PIA synthesis was markedly higher in *S. epidermidis* than in the *S. aureus* strains in vitro as well as in vivo. With both assays, it could be demonstrated that in vitro *ica* or PIA is expressed mainly during the stationary phase in *S. aureus* strain RN6390 but is repressed in strain Newman. Interestingly, the *ica* transcripts preceded the detected PIA production in vivo. This suggests a delay between the transcription and the biosynthesis of PIA. The synthesis of this β-1,6-linked *N*-acetylglucosamine polysaccharide is dependent on the supply of precursor molecules, which are processed by the enzymes encoded by the *ica* operon. Thus, besides the *ica*-encoded enzymes, the concentration of these precursor molecules is probably also crucial for overall PIA production. This hypothesis is supported by the *ica or* PIA expression analysis performed with *S. epidermidis* grown with and without glucose (10).

In the case of separate inoculation of wild-type and mutant strains, growth and adherence to catheters by *S. aureus* and *S. epidermidis* in vivo were not dependent on PIA expression. This observation is in agreement with previous observations by us and others (17, 31). Nevertheless, the role of PIA as a virulence factor of *S. epidermidis* has been demonstrated in two other animal models. In a central venous catheter-related infection model, the PIA-positive *S. epidermidis* strains adhered better to the implanted catheter and caused metastatic diseases more often than did the PIA-negative mutants (48, 50). In a foreign-body infection mouse model, subcutaneously implanted catheters infected with *S. epidermidis* 1457 formed abscesses more often and the number of recovered bacteria adhering on the plastic catheters was higher than that with the PIA-negative mutant (49). In this model, attachment of *S. epidermidis* occurred on the native implants. In contrast, in the animal model used here and by Francois et al. (17), tissue cages with catheter pieces were precoated with host proteins before bacterial inoculation. These coating proteins may impair the adherence of *S. epidermidis* since it was shown in vitro that plasma proteins, fibrinogen, and fibronectin decrease the binding of *S. epidermidis* to artificial surfaces (20, 25, 56). In contrast, *S. aureus* adherence to implants coated by host proteins is promoted by cell wall adhesins (15). This could explain the clinical observation that prosthetic implant infections due to *S. epidermidis* occur mainly during the surgical procedures, whereas *S. aureus* infections can occur hematogenously even years after the procedure.

Growth of wild-type strains and *ica* mutants was equal when the strains were injected separately. In contrast, in competition experiments where wild-type strains and *ica* mutants were injected together in a ratio of 1:1 into the same cages, the *ica* mutant strain reached lower bacterial numbers than the wild type. This observation suggests an attenuated virulence of the *ica* mutant compared to that of wild-type strains in the foreign-body model. In a recently published report, it was shown that in a mouse model of *Yersinia pseudotuberculosis*, the presence of wild-type bacteria severely hindered the ability of mutant strains to persist and colonize different tissues (33).

In conclusion, we show that the device-related animal model is suitable for studying the time course of biofilm formation in *S. aureus* and *S. epidermidis*. We demonstrated that in *S. epidermidis* infection, PIA is detectable early in the infection course and that PIA production is induced in *S. aureus* infection during the course of a device-related infection. PIA pro-

duction and biofilm formation are present in both species late in infection. Taken together, our results show that the *ica* locus and biofilm formation are crucial parameters for staphylococcal colonization and survival on implants.

ACKNOWLEDGMENTS

We thank Z. Rajacic for his expert technical assistance with the animal model and Heinz Schwarz for his excellent support with electron microscopy. We are grateful to Sarah Cramton and Fritz Götz for the *ica* gene replacement mutant of strain ATCC 35556.

This work was supported by grants from the Deutsche Forschungsgemeinschaft (Wo578/3-3 and Ma1522/4-3) and from the Stiftung für Infektionskrankheiten beider Basel.

The animals used in this study were kept in the Animal House of the Department of Research, University Hospital, Basel, Switzerland, and animal experimentation guidelines were followed according to the regulations of Swiss veterinary law.

REFERENCES

1. **Arciola, C. R., L. Baldassarri, and L. Montanaro.** 2001. Presence of *icaA* and *icaD* genes and slime production in a collection of staphylococcal strains from catheter-associated infections. J. Clin. Microbiol. **39:**2151–2156.
2. **Cheung, A. L., J. M. Koomey, C. A. Butler, S. J. Projan, and V. A. Fischetti.** 1992. Regulation of exoprotein expression in Staphylococcus aureus by a locus (sar) distinct from agr. Proc. Natl. Acad. Sci. USA **89:**6462–6466.
3. **Christensen, G. D., J. T. Parisi, A. L. Bisno, W. A. Simpson, and E. H. Beachey.** 1983. Characterization of clinically significant strains of coagulase-negative staphylococci. J. Clin. Microbiol. **18:**258–269.
4. **Christensen, G. D., W. A. Simpson, A. L. Bisno, and E. H. Beachey.** 1982. Adherence of slime-producing strains of *Staphylococcus epidermidis* to smooth surfaces. Infect. Immun. **37:**318–326.
5. **Christensen, G. D., W. A. Simpson, J. J. Younger, L. M. Baddour, F. F. Barrett, D. M. Melton, and E. H. Beachey.** 1985. Adherence of coagulase-negative staphylococci to plastic tissue culture plates: a quantitative model for the adherence of staphylococci to medical devices. J. Clin. Microbiol. **22:**996–1006.
6. **Conlon, K. M., H. Humphreys, and J. P. O'Gara.** 2002. *icaR* encodes a transcriptional repressor involved in environmental regulation of *ica* operon expression and biofilm formation in *Staphylococcus epidermidis*. J. Bacteriol. **184:**4400–4408.
7. **Cramton, S. E., C. Gerke, N. F. Schnell, W. W. Nichols, and F. Götz.** 1999. The intercellular adhesion (*ica*) locus is present in *Staphylococcus aureus* and is required for biofilm formation. Infect. Immun. **67:**5427–5433.
8. **Cramton, S. E., M. Ulrich, F. Götz, and G. Döring.** 2001. Anaerobic conditions induce expression of polysaccharide intercellular adhesin in *Staphylococcus aureus* and *Staphylococcus epidermidis*. Infect. Immun. **69:**4079–4085.
9. **de Silva, G. D. I., M. Kantzanou, A. Justice, R. C. Massey, A. R. Wilkinson, N. P. J. Day, and S. J. Peacock.** 2002. The *ica* operon and biofilm production in coagulase-negative staphylococci associated with carriage and disease in a neonatal intensive care unit. J. Clin. Microbiol. **40:**382–388.
10. **Dobinsky, S., K. Kiel, H. Rohde, K. Bartscht, J. K.-M. Knobloch, M. A. Horstkotte, and D. Mack.** 2003. Glucose-related dissociation between *icaADBC* transcription and biofilm expression by *Staphylococcus epidermidis*: evidence for an additional factor required for polysaccharide intercellular adhesin synthesis. J. Bacteriol. **185:**2879–2886.
11. **Donlan, R. M.** 2001. Biofilm formation: a clinically relevant microbiological process. Clin. Infect. Dis. **33:**1387–1392.
12. **Donlan, R. M.** 2002. Biofilms: microbial life on surfaces. Emerg. Infect. Dis. **8:**881–890.
13. **Duthie, E., and L. L. Lorenz.** 1952. Staphylococcal coagulase: mode of action and antigenicity. J. Gen. Microbiol. **6:**95–107.
14. **Fluckiger, U., C. Wolz, and A. L. Cheung.** 1998. Characterization of a *sar* homolog of *Staphylococcus epidermidis*. Infect. Immun. **66:**2871–2878.
15. **Foster, T. J., and M. Hook.** 1998. Surface protein adhesins of Staphylococcus aureus. Trends Microbiol. **6:**484–488.
16. **Fowler, V. G., Jr., P. D. Fey, L. B. Reller, A. L. Chamis, G. R. Corey, and M. E. Rupp.** 2001. The intercellular adhesin locus ica is present in clinical isolates of Staphylococcus aureus from bacteremic patients with infected and uninfected prosthetic joints. Med. Microbiol. Immunol. (Berlin) **189:**127–131.
17. **Francois, P., P. H. Tu Quoc, C. Bisognano, W. L. Kelley, D. P. Lew, J. Schrenzel, S. E. Cramton, F. Gotz, and P. Vaudaux.** 2003. Lack of biofilm contribution to bacterial colonisation in an experimental model of foreign body infection by Staphylococcus aureus and Staphylococcus epidermidis. FEMS Immunol. Med. Microbiol. **35:**135–140.
18. **Frebourg, N. B., S. Lefebvre, S. Baert, and J.-F. Lemeland.** 2000. PCR-based assay for discrimination between invasive and contaminating *Staphylococcus epidermidis* strains. J. Clin. Microbiol. **38:**877–880.
19. **Galdbart, J. O., J. Allignet, H. S. Tung, C. Ryden, and N. El Solh.** 2000. Screening for Staphylococcus epidermidis markers discriminating between skin-flora strains and those responsible for infections of joint prostheses. J. Infect. Dis. **182:**351–355.
20. **Galliani, S., A. Cremieux, P. van der Auwera, and M. Viot.** 1996. Influence of strain, biomaterial, proteins, and oncostatic chemotherapy on Staphylococcus epidermidis adhesion to intravascular catheters in vitro. J. Lab. Clin. Med. **127:**71–80.
21. **Gerke, C., A. Kraft, R. Sussmuth, O. Schweitzer, and F. Gotz.** 1998. Characterization of the N-acetylglucosaminyltransferase activity involved in the biosynthesis of the Staphylococcus epidermidis polysaccharide intercellular adhesin. J. Biol. Chem. **273:**18586–18593.
22. **Goerke, C., M. G. Bayer, and C. Wolz.** 2001. Quantification of bacterial transcripts during infection using competitive reverse transcription-PCR (RT-PCR) and LightCycler RT-PCR. Clin. Diagn. Lab. Immunol. **8:**279–282.
23. **Goerke, C., S. Campana, M. G. Bayer, G. Döring, K. Botzenhart, and C. Wolz.** 2000. Direct quantitative transcript analysis of the *agr* regulon of *Staphylococcus aureus* during human infection in comparison to the expression profile in vitro. Infect. Immun. **68:**1304–1311.
24. **Goerke, C., U. Fluckiger, A. Steinhuber, W. Zimmerli, and C. Wolz.** 2001. Impact of the regulatory loci agr, sarA and sae of Staphylococcus aureus on the induction of alpha-toxin during device-related infection resolved by direct quantitative transcript analysis. Mol. Microbiol. **40:**1439–1447.
25. **Gotz, F., and G. Peters.** 2000. Colonization of medical devices by coagulase-negative staphylococci, p. 55–88. *In* F. A. Waldvogel and A. L. Bisno (ed.), Infections associated with indwelling medical devices, 3rd ed. American Society for Microbiology, Washington, D.C.
26. **Heilmann, C., M. Hussain, G. Peters, and F. Gotz.** 1997. Evidence for autolysin-mediated primary attachment of Staphylococcus epidermidis to a polystyrene surface. Mol. Microbiol. **24:**1013–1024.
27. **Heilmann, C., O. Schweitzer, C. Gerke, N. Vanittanakom, D. Mack, and F. Gotz.** 1996. Molecular basis of intercellular adhesion in the biofilm-forming Staphylococcus epidermidis. Mol. Microbiol. **20:**1083–1091.
28. **Jefferson, K. K., S. E. Cramton, F. Gotz, and G. B. Pier.** 2003. Identification of a 5-nucleotide sequence that controls expression of the ica locus in Staphylococcus aureus and characterization of the DNA-binding properties of IcaR. Mol. Microbiol. **48:**889–899.
29. **Knobloch, J. K.-M., K. Bartscht, A. Sabottke, H. Rohde, H.-H. Feucht, and D. Mack.** 2001. Biofilm formation by *Staphylococcus epidermidis* depends on functional RsbU, an activator of the *sigB* operon: differential activation mechanisms due to ethanol and salt stress. J. Bacteriol. **183:**2624–2633.
30. **Knobloch, J. K.-M., M. A. Horstkotte, H. Rohde, and D. Mack.** 2002. Evaluation of different detection methods of biofilm formation in Staphylococcus aureus. Med. Microbiol. Immunol. (Berlin) **191:**101–106.
31. **Kristian, S. A., T. Golda, F. Ferracin, S. E. Cramton, B. Neumeister, A. Peschel, F. Gotz, and R. Landmann.** 2004. The ability of biofilm formation does not influence virulence of Staphylococcus aureus and host response in a mouse tissue cage infection model. Microb. Pathog. **36:**237–245.
32. **Kristian, S. A., X. Lauth, V. Nizet, F. Goetz, B. Neumeister, A. Peschel, and R. Landmann.** 2003. Alanylation of teichoic acids protects Staphylococcus aureus against Toll-like receptor 2-dependent host defense in a mouse tissue cage infection model. J. Infect. Dis. **188:**414–423.
33. **Logsdon, L. K., and J. Mecsas.** 2003. Requirement of the *Yersinia pseudotuberculosis* effectors YopH and YopE in colonization and persistence in intestinal and lymph tissues. Infect. Immun. **71:**4595–4607.
34. **Mack, D., K. Bartscht, S. Dobinsky, M. A. Horstkotte, K. Kiel, J. K. Knobloch, and P. Schäfer.** 2000. Staphylococcal factors involved in adhesion and biofilm formation on biomaterials, p. 307–330. *In* Y. H. An and R. J. Friedman (ed.), Handbook for studying bacterial adhesion: principles, methods, and applications. Humana Press Inc., Totowa, N.J.
35. **Mack, D., W. Fischer, A. Krokotsch, K. Leopold, R. Hartmann, H. Egge, and R. Laufs.** 1996. The intercellular adhesin involved in biofilm accumulation of *Staphylococcus epidermidis* is a linear β-1,6-linked glucosaminoglycan: purification and structural analysis. J. Bacteriol. **178:**175–183.
36. **Mack, D., M. Nedelmann, A. Krokotsch, A. Schwarzkopf, J. Heesemann, and R. Laufs.** 1994. Characterization of transposon mutants of biofilm-producing *Staphylococcus epidermidis* impaired in the accumulative phase of biofilm production: genetic identification of a hexosamine-containing polysaccharide intercellular adhesin. Infect. Immun. **62:**3244–3253.
37. **Mack, D., J. Riedewald, H. Rohde, T. Magnus, H. H. Feucht, H.-A. Elsner, R. Laufs, and M. E. Rupp.** 1999. Essential functional role of the polysaccharide intercellular adhesin of *Staphylococcus epidermidis* in hemagglutination. Infect. Immun. **67:**1004–1008.
38. **Mack, D., H. Rohde, S. Dobinsky, J. Riedewald, M. Nedelmann, J. K.-M. Knobloch, H.-A. Elsner, and H. H. Feucht.** 2000. Identification of three essential regulatory gene loci governing expression of *Staphylococcus epidermidis* polysaccharide intercellular adhesin and biofilm formation. Infect. Immun. **68:**3799–3807.
39. **Mack, D., N. Siemssen, and R. Laufs.** 1992. Parallel induction by glucose of adherence and a polysaccharide antigen specific for plastic-adherent *Staph-*

ylococcus epidermidis: evidence for functional relation to intercellular adhesion. Infect. Immun. **60:**2048–2057.
40. **Martín-López, J. V., E. Pérez-Roth, F. Claverie-Martín, O. Díez Gil, N. Batista, M. Morales, and S. Méndez-Álvarez.** 2002. Detection of *Staphylococcus aureus* clinical isolates harboring the *ica* gene cluster needed for biofilm establishment. J. Clin. Microbiol. **40:**1569–1570.
41. **McKenney, D., K. L. Pouliot, Y. Wang, V. Murthy, M. Ulrich, G. Doring, J. C. Lee, D. A. Goldmann, and G. B. Pier.** 1999. Broadly protective vaccine for Staphylococcus aureus based on an in vivo-expressed antigen. Science **284:**1523–1527.
42. **Muller, E., S. Takeda, H. Shiro, D. Goldmann, and G. B. Pier.** 1993. Occurrence of capsular polysaccharide/adhesin among clinical isolates of coagulase-negative staphylococci. J. Infect. Dis. **168:**1211–1218.
43. **Novick, R.** 1991. Genetic systems in staphylococci. Methods Enzymol. **204:** 587–636.
44. **Peacock, S. J., C. E. Moore, A. Justice, M. Kantzanou, L. Story, K. Mackie, G. O'Neill, and N. P. J. Day.** 2002. Virulent combinations of adhesin and toxin genes in natural populations of *Staphylococcus aureus*. Infect. Immun. **70:**4987–4996.
45. **Peng, H. L., R. P. Novick, B. Kreiswirth, J. Kornblum, and P. Schlievert.** 1988. Cloning, characterization, and sequencing of an accessory gene regulator (agr) in *Staphylococcus aureus*. J. Bacteriol. **170:**4365–4372.
46. **Rachid, S., K. Ohlsen, U. Wallner, J. Hacker, M. Hecker, and W. Ziebuhr.** 2000. Alternative transcription factor σ^B is involved in regulation of biofilm expression in a *Staphylococcus aureus* mucosal isolate. J. Bacteriol. **182:**6824–6826.
47. **Rohde, H., J. K. Knobloch, M. A. Horstkotte, D. Mack, C. R. Arciola, L. Montanaro, and L. Baldassarri.** 2001. Correlation of *Staphylococcus aureus icaADBC* genotype and biofilm expression phenotype. J. Clin. Microbiol. **39:**4595–4596.
48. **Rupp, M. E., P. D. Fey, C. Heilmann, and F. Gotz.** 2001. Characterization of the importance of Staphylococcus epidermidis autolysin and polysaccharide intercellular adhesin in the pathogenesis of intravascular catheter-associated infection in a rat model. J. Infect. Dis. **183:**1038–1042.
49. **Rupp, M. E., J. S. Ulphani, P. D. Fey, K. Bartscht, and D. Mack.** 1999. Characterization of the importance of polysaccharide intercellular adhesin/hemagglutinin of *Staphylococcus epidermidis* in the pathogenesis of biomaterial-based infection in a mouse foreign body infection model. Infect. Immun. **67:**2627–2632.
50. **Rupp, M. E., J. S. Ulphani, P. D. Fey, and D. Mack.** 1999. Characterization of *Staphylococcus epidermidis* polysaccharide intercellular adhesin/hemagglutinin in the pathogenesis of intravascular catheter-associated infection in a rat model. Infect. Immun. **67:**2656–2659.
51. **Tsukayama, D. T., R. Estrada, and R. B. Gustilo.** 1996. Infection after total hip arthroplasty. A study of the treatment of one hundred and six infections. J. Bone Joint Surg. Am. **78:**512–523.
52. **Valle, J., A. Toledo-Arana, C. Berasain, J. M. Ghigo, B. Amorena, J. R. Penades, and I. Lasa.** 2003. SarA and not sigmaB is essential for biofilm development by Staphylococcus aureus. Mol. Microbiol. **48:**1075–1087.
53. **Vuong, C., C. Gerke, G. A. Somerville, E. R. Fischer, and M. Otto.** 2003. Quorum-sensing control of biofilm factors in Staphylococcus epidermidis. J. Infect. Dis. **188:**706–718.
54. **Wolz, C., C. Goerke, R. Landmann, W. Zimmerli, and U. Fluckiger.** 2002. Transcription of clumping factor A in attached and unattached *Staphylococcus aureus* in vitro and during device-related infection. Infect. Immun. **70:** 2758–2762.
55. **Wolz, C., D. McDevitt, T. J. Foster, and A. L. Cheung.** 1996. Influence of *agr* on fibrinogen binding in *Staphylococcus aureus* Newman. Infect. Immun. **64:**3142–3147.
56. **Zdanowski, Z., E. Ribbe, and C. Schalen.** 1993. Influence of some plasma proteins on in vitro bacterial adherence to PTFE and Dacron vascular prostheses. APMIS **101:**926–932.
57. **Ziebuhr, W., C. Heilmann, F. Götz, P. Meyer, K. Wilms, E. Straube, and J. Hacker.** 1997. Detection of the intercellular adhesion gene cluster (*ica*) and phase variation in *Staphylococcus epidermidis* blood culture strains and mucosal isolates. Infect. Immun. **65:**890–896.
58. **Zimmerli, W., and P. E. Ochsner.** 2003. Management of infection associated with prosthetic joints. Infection **31:**99–108.
59. **Zimmerli, W., F. A. Waldvogel, P. Vaudaux, and U. E. Nydegger.** 1982. Pathogenesis of foreign body infection: description and characteristics of an animal model. J. Infect. Dis. **146:**487–497.

Editor: A. D. O'Brien